Preprints are preliminary reports that have not undergone peer review.
They should not be considered conclusive, used to inform clinical practice,
or referenced by the media as validated information.

Hydroxy Acid Conjugation to Lipids Increases Structural and Hydrolytic Stability

Moran Frenkel-Pinter

`moran.frenkel-pinter@mail.huji.ac.il`

The Hebrew University of Jerusalem https://orcid.org/0000-0001-7235-5845

Rotem Edri

The Hebrew University of Jerusalem

Yael Levi-Kalisman

The Hebrew University of Jerusalem https://orcid.org/0000-0002-2764-2738

Sarah Fisher

The Hebrew University of Jerusalem

Article

Keywords: self-assembly, hydrolysis, chemical evolution, origins of life, prebiotic chemistry, water chemistry

Posted Date: December 16th, 2025

DOI: https://doi.org/10.21203/rs.3.rs-5922500/v1

License: 🅭 🅯 This work is licensed under a Creative Commons Attribution 4.0 International License.
Read Full License

Additional Declarations: There is **NO** Competing Interest.

Hydroxy Acid Conjugation to Lipids Increases Structural and Hydrolytic Stability

R. Edri[1], S. Fisher[1], Y. Levi-Kalisman[2], and M. Frenkel-Pinter[1,2]*

[1] Institute of Chemistry, The Hebrew University of Jerusalem, Israel 9190401

[2] The Center for Nanoscience and Nanotechnology, The Hebrew University of Jerusalem, Israel 9190401

*Corresponding author:

Dr. Moran Frenkel-Pinter
The Center for Nanoscience and Nanotechnology
Institute of Chemistry
The Hebrew University of Jerusalem
Edmond J. Safra Campus
Jerusalem 9190401, Israel
Ph: (+972)-2-6584171
moran.fp@mail.huji.ac.il

KEYWORDS: self-assembly, hydrolysis, chemical evolution, origins of life, prebiotic chemistry, water chemistry

Abstract

Contemporary life requires functional polymers and phospholipid-derived compartmentalization. Mutualistic relationships between compartmentalization and polymerization have never been demonstrated in an abiotic scenario. As both the polymerization of hydroxy acids and the primitive cell-like aggregation of short-chain fatty acids are well known, we studied cooperative interactions between compartmentalization and polymerization using these two classes of molecules as a model system. To that end, we explored the formation of various hydroxy acid-fatty acid conjugates. All reactions produced two types of condensation products: hydroxy acid homoesters and lipid-hydroxy acid heteroesters. We found that conjugation of hydroxy acids to fatty acids led to the reduction of fatty acid critical aggregation concentration by an order of magnitude. Furthermore, hydroxy acid oligomers were protected against hydrolysis only upon conjugation to fatty acids. Our work offers meaningful insights into the role of self-assembly and cooperative chemistry as selective driving forces in lipid-polymer co-evolution.

Introduction

One of the puzzling questions in origins of life research is which pathways might allow the coupling of compartmentalization and polymerization.[1] The existence of compartments is essential in promoting Darwinian evolution, forming microenvironments in which cellular chemistry can occur.[2,3] In the prebiotic context, compartmentalization offers physical mechanisms to promote polymerization by localizing different building blocks at high concentration and in close proximity. Compartmentalization can also hinder polymer hydrolysis, which is thermodynamically favorable in aqueous environments. In modern biology, the role of compartmentalization is exclusively played by phospholipids, the key building blocks of cell membranes.[4] Membranes formed by the self-aggregation of phospholipids and other contemporary lipids possess low permeability and physical durability, allowing the membranes to act as selective barriers.[5] Such properties, while desirable from a biological perspective, may raise difficulties in the context of prebiotic environments, wherein greater diffusion of small molecules through the membrane was likely necessary in the absence of highly evolved specific membranal transporters. Furthermore, the chemical nature and complexity of phospholipids may suggest that they are the products of prolonged evolution.

The core building blocks of phospholipids, fatty acids, are found in model prebiotic reactions via Fischer–Tropsch type synthesis [6-8] and are abundant in meteorites, [9,10] although they are considerably shorter than the fatty acids found in contemporary phospholipids. Despite the high complexity of phospholipids, several prebiotic routes for their synthesis have been suggested.[11] These include using activated fatty acids and phosphoglycerol, [12] transacylation of lysophospholipids and acyl thioesters,[13] as well as transacylation of *N*-acyl imidazole and glycerol 3-phosphocholine.[14] Recently, researchers described a novel prebiotic synthesis of complex lysophospholipid derivatives harboring amino-alcohol phospholipids as a head group. These were synthesized by the reaction of 1-decanoyl glycerol-2,3-with cyclic phosphate and 2-amino alcohols.[15]

In addition to chemically-modified amphiphiles, single-chain prebiotically plausible amphiphiles such as medium-chain fatty acids (C8-C12) are considered natural protocell building blocks.[16] The self-assembly of such molecules into vesicles has been thoroughly studied.[17-20] Although considered more prebiotic than phospholipids, vesicles formed by simple fatty acids suffer from poor physical stability and high permeability, and they are sustained under very limited set of conditions: a narrow range of pH levels and temperatures and low salinity. Moreover, fatty acids are extremely sensitive to divalent cations, such as magnesium ions, which are essential for RNA folding.[21] Despite these limitations, cooperative aggregation and the presence of other building blocks help to stabilize fatty acid vesicles. For example, the presence of even small amounts of fatty alcohols, mono-acyl glycerides, and alkylamines reduces the critical vesicle concentration (CVC) and stabilizes decanoic acid vesicles at a wider range of pH conditions and over a greater range of salt concentrations.[18,22,23] Amino acids, peptides, nucleobases, and sugars also stabilize decanoic acid vesicles, and studies have demonstrated that some inhibit flocculation in the presence of electrolytes via noncovalent interactions.[24-28] Alternative prebiotic amphiphiles have been suggested.[29-32]

The molecular diversity on Early Earth was immense, and included various organic molecules that were either delivered exogenously by meteorites or produced from fundamental building blocks in situ.[33,34] Among them, hydroxy acids (HAs) are highly attractive molecules in the context of origins of life; they serve as metabolites in extant biology, exhibit high reactivity, and play a catalytic role in prebiotic peptide synthesis.[35] HAs such as glycolic acid and lactic acid have been found to facilitate peptide bond formation via ester-amide exchange under wet-dry cycling and drying reactions.[36,37] Polyesters formed by the polymerization of various HAs under drying conditions aggregate into microdroplets and are capable of compartmentalization.[38-40] All biopolymers result from condensation-dehydration reactions and can hydrolyze in water. [41,42] Hence, in a prebiotic context, formation of polymers by itself is insufficient, and strategies to impart hydrolytic stability are perhaps of equivalent importance. Therefore, it is important to unravel plausible molecular mechanisms that enable simultaneous polymerization, hindered hydrolysis, and compartmentalization.

In this paper, we focused on studying the interplay between compartmentalization, polymerization, and hydrolysis, using a fatty acid-hydroxy acid model system. To that end, we investigated the formation of novel prebiotic amphiphiles obtained by reacting decanoic acid (DA) with four different HAs. Under simple drying conditions, we were able to produce a wide variety of lipid products which were characterized via various analytical and structural techniques. Our results indicate that DA is mostly reactive towards lactic acid, although heteroester products comprised of DA and HAs were obtained for all tested HAs. Moreover, we studied the cooperative interactions between the two classes of molecules. Our results indicate synergistic interactions and pure molecular mutualism, where on one hand, conjugation of hydroxy acids to lipids promoted greater self-assembly propensity of the lipids, and on the other hand, this conjugation protected hydroxy acid esters from hydrolysis. These results highlight the importance of cooperative interactions between different classes of molecules in shaping early chemical evolution.

Results and discussion

Drying reactions between decanoic acid and hydroxy acids.

The prebiotic molecular inventory was highly rich in short- to medium-chain fatty acids (up to 10-12-carbon long chains are considered abundant) as well as other simple organic molecules such as hydroxy acids (HAs). We investigated esterification reactions between decanoic acid (10-carbon long fatty acid, DA) and four different HAs: glycolic acid (GA), L-lactic acid (LA), L-malic acid (MA), and L-phenyllactic acid (PLA) (Figure 1), to produce the *O*-acylhydroxy acids. Decanoic acid and single HAs (either GA, LA, MA, or PLA) were allowed to react under dry conditions for 7 days at 85°C at a 1:1, 1:2, and 1:4 molar ratio (in favor of the HAs). Following the reaction, we analyzed the resulting products via LC-UV-MS, FTIR, and NMR. We found that all four HAs reacted to produce either homoesters (oligomers of pure HAs) or heteroesters containing HAs-DA conjugates (Figure 2A-B). For all HAs tested, the HAs-DA conjugates contained one DA and n-HAs, as expected. Typically, the number of products and their concentration (both homoesters and heteroesters) increased as the amount of the HA increased, with the exception of PLA, for which no significant differences were observed as the molar ratio increased (Figures S1-S21).

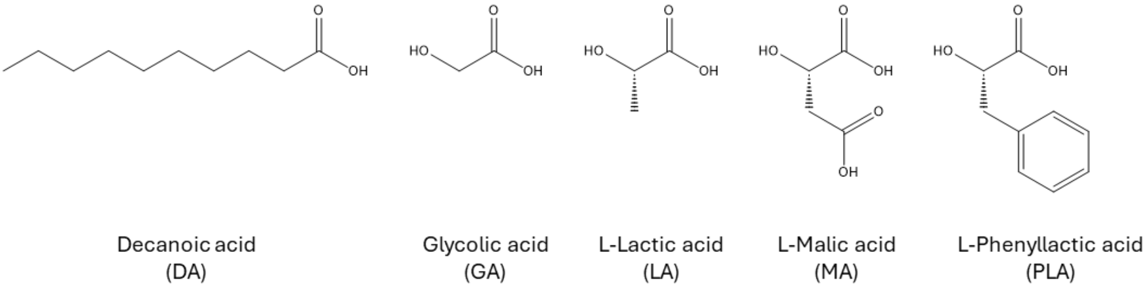

Figure 1. Chemical structure and abbreviations of the studied monomers. Mixtures of decanoic acid and one of the four alpha hydroxy acids were allowed to react at 85˚C for 7 days under dry conditions to produce homoesters or heteroesters.

The identification of oligomer length and composition was achieved using LC-MS (Figure 2C-D, Figures S22-S155, Tables S1-S9). Out of the four tested HAs we found that LA produced the longest heteroesters (12LA1DA) while GA, PLA, and MA produced similar length oligomers of up to 5-6 HA. As for homoesters, GA produced the longest oligomers (16GA) and LA, MA, and PLA produced up to 13-,12-, and 7- mers, respectively. Interestingly, in the absence of DA, LA oligomerized to form products of up 18 mers and possibly longer species (Tables S4-S6, Figures S72-S124), suggesting that the formation of DA-LA heteroesters came at the expense of LA homoesters. The formation of the esterification products was further confirmed by FTIR (Figures S156-S164) and NMR measurements (Figures S165-S185). Shift in the carbonyl stretching in FTIR and down-field shift of the alpha protons in NMR indicated that ester bonds were formed in all tested mixtures upon drying.

We measured the conversion of DA into products in the various reactions via HPLC and found that the highest consumption was observed when DA reacted with LA, followed by PLA, GA, and MA. DA conversion was dependent on the DA:HA ratio: as the ratio increased, the DA conversion also increased. For instance, the consumption of DA when reacted with GA at a 1:1 molar ratio was 18±2%, while at a 1:4 molar ratio the conversion was 24±3%. One exception was the case of MA, for which DA conversion was constant regardless of the amount of MA, at around 15%. The highest conversion of DA was observed for reactions with LA, with a 29±1%, a 40±2%, and a 54±1% conversion at 1:1, 1:2, and 1:4 molar ratios, respectively (Figure S186).

The reactivity of DA towards esterification seemed to be dictated mostly by the chemical nature of the HA. Less hydrophilic HAs such as LA and PLA (logP of -0.72 and 1.01 respectively) appeared to facilitate the conversion of DA with up to 54% and 32% conversion. On the other hand, the more hydrophilic HAs, GA and MA (logP of -1.1), reacted with DA to a lesser extent. Other factors such as steric hindrance and acid strength, which were found to affect the consumption of amino acids in depsipeptides formation,[36] were relatively negligible.[17,43] An additional factor that may affect the extent to which DA reacted with HAs is the physical state of the HA under reaction conditions. Among the four HAs, GA, MA, and PLA were introduced as solids while LA was a concentrated solution. Under reaction conditions, GA remained in the liquid state as well as LA. However, MA and PLA remained in the solid state and therefore their mobility was lower. While the physical state in the case of MA did not prevent homo-oligomerization of MA, it may inhibit PLA homo-oligomerization, as indicated in the control PLA sample (Figure S17). Remarkably, the conversion of PLA and the formation of the PLA homoesters in the presence of DA was significantly greater than the control sample (in the absence of DA) (Figure S187-188). A possible explanation for the positive effect of DA on PLA oligomerization may suggest that DA serves as a solvent, allowing partial solubility of PLA; consequently, PLA molecules became more mobile and thus reacted to a greater extent. It is possible that the oligomerization also took place at the solid-liquid interface formed by both PLA and DA molecules.

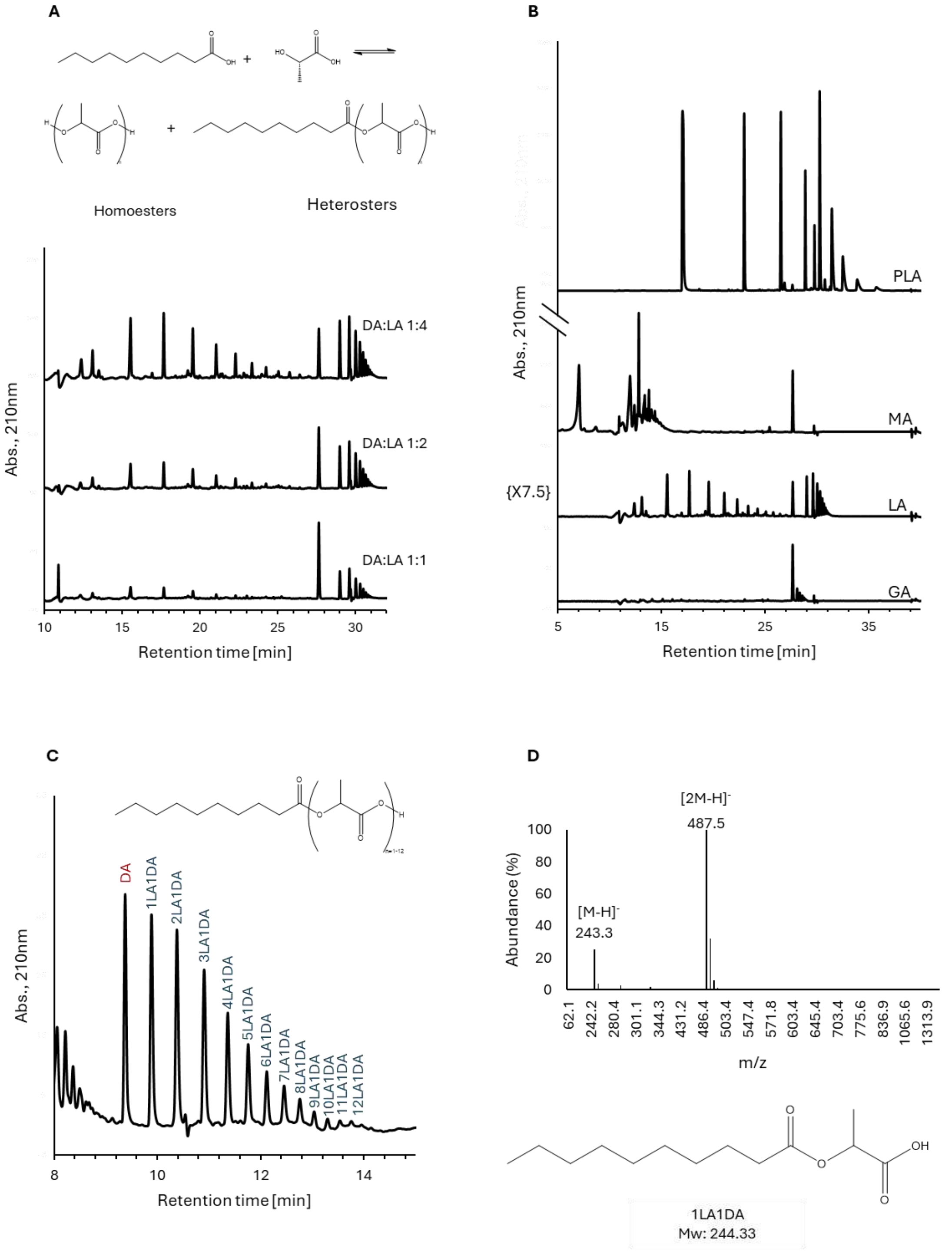

Figure 2. Novel amphiphiles derived from DA-HA conjugates were prebiotically synthesized under simple dry conditions. HPLC chromatograms were obtained for DA:LA reaction products at 1:1, 1:2, and 1:4 molar ratios. Two types of products including LA homoesters and DA-LA heteroesters were formed (A). HPLC chromatograms were obtained for DA:HA reaction products at 1:4 molar ratio (DA:HA) for the four tested HAs (B). HPLC chromatogram obtained for DA:LA reaction product at 1:4 molar ratio. The labeled signals are heteroesters of DA-LA$_n$ with up to 12LA-mers conjugated to DA (C). MS spectrum (negative mode) was obtained for the identification of 1LA1DA reaction product. The obtained m/z values correspond to [M-H]$^-$ and [2M-H]$^-$ ions (D).

Structural characterization of the reaction products.

Subsequently, we sought to study the assembly profile of DA-HA reaction products and observed distinct structural features in all reaction products. Decanoic acid is well known to form different types of structures depending on the pH, temperature, and concentration.[17,43,44] At pH levels around DA pKa (~7), where the molar ratio between the protonated decanoic acid and the charged, deprotonated decanoate species is about 1:1, vesicles form (commonly achieved within the range of pH 6.6-8.0).[45] At higher pH levels, at which most of the DA is in deprotonated form (i.e., decanoate anions), micelles form. At pH levels much lower than the pKa, most of the decanoic acid is in the neural protonated form and forms either oil droplets or solid precipitates, depending on temperature.[44] We sought to study the complex reaction mixture as a whole rather than isolated reaction products, in accordance with recent studies in systems chemistry.[46-50] We expected that the physical properties of the system will be affected by interconnected interactions between all components within the system. To study how the presence of a DA-HA reaction products affects the structure formation, we rehydrated the reaction products of DA and each of the four HAs in a 50 mM phosphate buffer and adjusted the pH to 6.8, at which vesicles are expected to form. The obtained samples were visually inspected and characterized by turbidity measurements and fluorescence microscopy. As indicated by both turbidity measurements and visual observations, most of the samples exhibited turbidity to some extent, suggesting that structures formed upon the rehydration process (Figures S189-S190).

Turbidity correlates with the light scattered from the sample, which depends on the structures present in the sample. Accordingly, turbidity measurements give a good indication of both structure size and distribution.[51] There was not a clear correlation between turbidity and the DA:HA molar ratio; indeed, each HA exhibited different behavior. For instance, while no significant differences in turbidity were observed for GA, in the case of LA, turbidity significantly decreased as the ratio increased in favor of LA. We further confirmed structure formation under a fluorescent microscope using rhodamine dye. The resulting rehydrated products consisted of DA at concentrations varying from 23mM to 43mM (Figure S191), which is above DA's critical vesicle concentration (CVC) at pH 6.8 (10-12mM).[19] Indeed, under the microscope, we were able to observe structures with distinct vesicle bilayers for most of the samples (Figure S192). However, the lipid bilayer was not clearly visualized for all samples, as in the case of LA-DA products. As expected, an abundance of giant vesicles of several microns in diameter correlated with increased turbidity of the samples. Samples of lower turbidity were visualized under a fluorescent microscope, but no clear image of their bilayer membrane was observed.

The particular case of LA-DA mixture is distinct within the scope of the experiment in both chemical and structural perspectives. Therefore, we conducted a more detailed characterization of this system. To understand how homoester and heteroester formation affected the observed structure formation, we prepared control samples of DA and LA fresh monomers at 1:1, 1:2, and 1:4 molar ratios, fixing DA concentration at 50 mM. The control samples were further characterized by turbidity measurements and fluorescence microscopy (Figure 3). In the case of the control monomer samples, as the HA:DA ratio increased, the turbidity of the samples increased (Figure 3A-B). Under the microscope, vesicles were clearly observed for all samples. However, the abundance of larger and deformed vesicles positively correlated with high LA concentrations. When comparing these observations to the reaction products, the opposite trend is observed. Namely, at a lower DA:LA molar ratio, the turbidity of the samples increased, and larger structures were detected under the microscope. Yet, as the ratio increased to 1:2 and 1:4 in favor of LA, the turbidity of the reaction products significantly decreased and less structures of larger size were observed under the microscope (Figure 3C). Since the concentration of monomeric DA decreased significantly in the reaction, we further prepared control samples consisting of DA at the concentration measured in the reaction products. Indeed, turbidity was slightly lower as DA concentration decreased. However, the abundance of structures was relatively high compared to the reaction products, mostly the ones for DA:LA 1:2 and 1:4 molar ratios (Figures S193-S194). These results suggest that the self-assembly properties of the systems were affected by the presence of the new products.

The reaction products were composed of two types of oligomers, LA homoesters and LA-DA heteroesters, leading us to examine the individual contribution of each type of product to the observed assemblies. For that purpose, we prepared a mixture of DA and LA homoesters (obtained by drying LA in the absence of DA) by rehydrating the LA reaction product in the presence of 50 mM DA at pH 6.8. As a control, we also rehydrated LA reaction products in the absence of DA. We found that both samples were turbid to some extent, while in the absence of DA, the LA esters exhibited significant inhomogeneity. Under a fluorescent microscope, the samples consisting of DA and LA homoesters without DA-LA heteroesters were found to form vesicles of various sizes for which the membrane was visualized. Aggregates related to LA oligomers were also observed (Figures S195). Interestingly, the samples in the absence of DA formed aggregates that were not dyed by rhodamine. This observation highlights the fact that DA molecules tend to be adsorbed at the surface of LA aggregates, resulting in their dying by rhodamine. The absence of LA aggregates in the combined DA-LA reaction products might be due to the presence of DA-LA conjugates that interfere with LA oligomer's aggregation. Alternatively, aggregates of LA oligomers may be formed only for minimum oligomer length. As mentioned previously, LA oligomerizes to form shorter homoesters of up to 13-mers in the presence of DA (Table S4, Figures S72-S89). However, in the absence of DA, LA oligomers reached 18-mers (Table S6, Figures S102-

S124). It may be possible that only oligomers of the longest chain length form such aggregates.

To further characterize the structures that were formed, we conducted cryogenic transmission electron microscopy (cryo-TEM) measurements for DA-LA reaction products and control samples at pH 6.8 (Figure 4). In all the reaction products, vesicles were detected (Figure S196). At 1:1 DA:LA molar ratio, large vesicles of varied lamellarity (both unilamellar vesicles (ULVs) and multilamellar vesicles (MLVs)) were observed, similarly to DA control. As the DA:LA ratio increased to 1:2 and 1:4, vesicle abundance decreased, consistent with the fluorescence microscopy results and the portion of ULVs increased. Surprisingly, at a 1:4 molar ratio of DA:LA, we were able to detect small ULVs, as well as tiny structures (dark dots of about 4-6nm), which we attribute to micelles (Figure 4D). The formation of micelles at this pH is not related solely to DA but probably to either the reaction products of DA and LA or to the co-aggregation of both DA remaining monomers and its LA derivatives. Indeed, esters of LA and fatty acid salts have been reported to form micelles at concentration levels of 1-83 mM, depending on fatty acid chain length.[52] These products consist of an anionic, carboxylic acid head group with a pKa lower than that of DA due to the adjacent ester group. Accordingly, at pH 6.8, most of the DA-LA conjugates are ionized and tend to form micelles rather than vesicles. The samples are composed of a mixture of at least 10 different amphiphiles, and accordingly it is likely that co-aggregates of the different amphiphiles are present. The possible formation of micelles may be essential for promoting catalytic activity and inducing protocellular fission, as previous studies have shown.[53-55]

Vesicles were also observed in the control samples of fresh monomers, however the nature of these vesicles differed (Figure 4A and 4B). Overall, the vesicles observed for the fresh samples were more heterogeneous in terms of size and lamellarity. Remarkably, the shape of the vesicles gradually changed as the DA:LA ratio increased (Figure S196). While at a 1:1 molar ratio of DA:LA most of the vesicles were spherical, at a 1:2 molar ratio some of the vesicles appeared partially deformed. This was much more prominent at a 1:4 molar ratio, at which ill-defined membranous structures were observed (Figure 4A and 4B). Overall, the structural properties of the fresh monomers and the reaction products differed significantly, exhibiting different structures and varied size distribution.

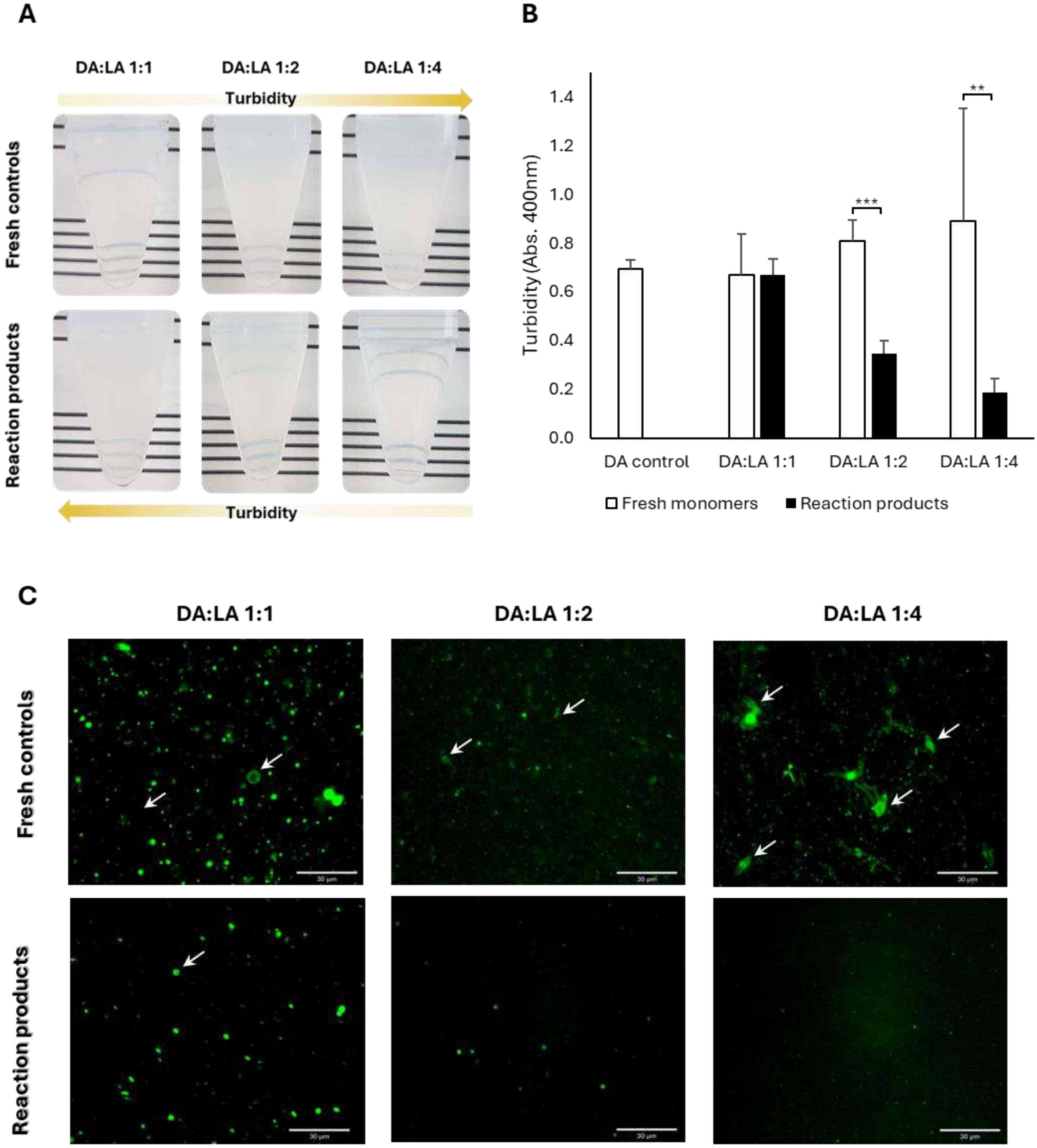

Figure 3. Characterization of DA-LA mixtures reveals structural differences between fresh monomers and reaction products. All samples were prepared in a phosphate buffer (50mM) at pH 6.8. The concentration of DA was 50 mM, and the concentration of LA was either 50, 100, or 200mM. In the case of the reaction products, DA and LA concentrations refer to the initial amounts prior to the reaction. Visual appearance of DA-LA mixtures of fresh monomers (top) or reaction products (bottom) (A). Turbidity (measured as the absorption at 400nm) of DA-LA mixtures of fresh monomers (white columns) and reaction products (black columns). As indicated by the turbidity measurements, opposing trends were observed for the fresh monomers and the reaction products. While an increase in LA concentration resulted in increased turbidity in the case of the fresh monomers (not statistically significant), the turbidity significantly decreased in the case of the reaction products ($p<0.001$). The effects were not significant for DA:LA 1:1 molar ratio, however at 1:2 and 1:4 the differences in turbidity were significant ($p<0.001$ and $p< 0.05$ respectively). T-test was used to determine statistical significance (B). Fluorescent microscopy images (x60 magnification) of DA-LA fresh monomers (top) or reaction products (bottom). Rhodamine 6G was used as a fluorescent probe. Structures were formed in all tested samples, as indicated by the images. Vesicles, indicated by the dying of the membrane (labeled with white arrows), were detected in all samples with the exceptions of DA:LA reaction products at 1:2 and 1:4 molar ratios, for which no clear images of the membrane were detected (C).

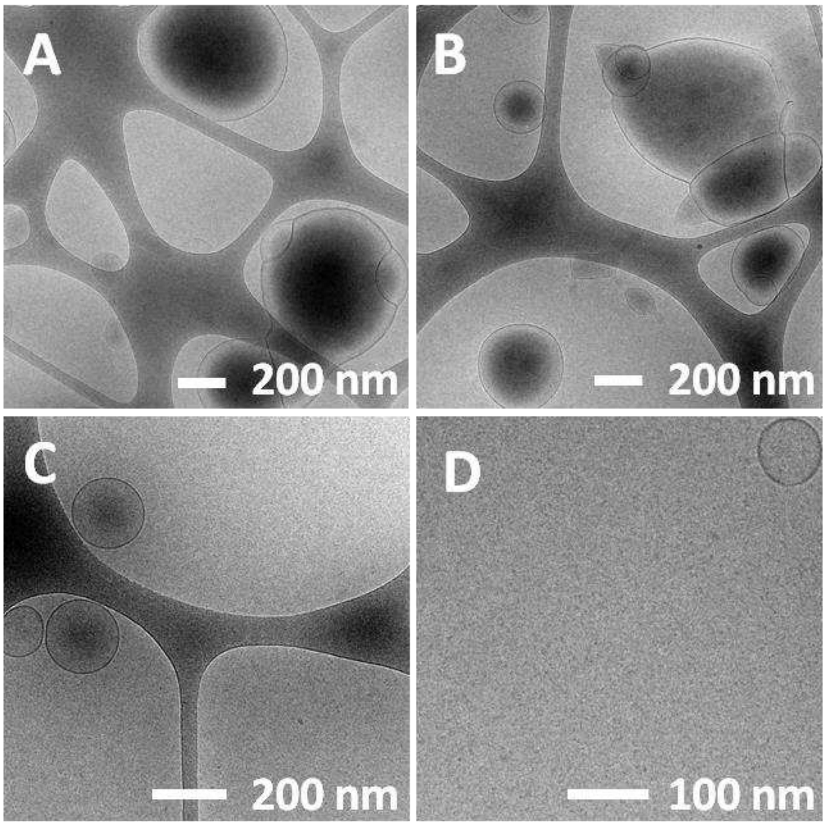

Figure 4. Cryo-TEM images of DA:LA fresh monomers (A, B) and reaction products (C, D) at 1:4 molar ratio. Cryo-TEM images confirm the formation of spherical and ill-defined membranous structures in the fresh monomers. In the reaction products we observed vesicles that were almost exclusively of the unilamellar subtype, and mostly less than 200 nm in size. Many small dots, mostly of about 4-6 nm, were also observed, which we attribute to micellar structures.

The DA-LA reaction products were found to have a tremendous impact on DA self-assembly properties, leading us to postulate that the conjugation of LA to DA will affect its effective aggregation concentration. To test this hypothesis, we measured the CAC of DA or DA-LA reaction products at pH 6.8. We used merocyanine 540 (MC540) assay to determine the critical aggregation concentration (CAC) of DA. Notably, the MC540 assay is not selective towards certain aggregation and can be used for CAC determination of various aggregates, including vesicles and micelles.[56,57] As demonstrated in Figure 5 and Figure S197, the CAC of DA at 50 mM phosphate buffer at pH 6.8 was found to be ca. 10 mM, which is in agreement with previous studies.[19] The impact of the DA-LA reaction products on DA's CAC was dramatic. As the DA:LA molar ratio in the drying reaction increased, the CAC of resulting products decreased, reaching concentrations of about 4.7 mM, 2.0 mM, and 1.0 mM at 1:1, 1:2, and 1:4 molar ratios of DA:LA respectively (Figure 5 and Figures S198-S200). This corresponds to 2-, 5-, and 10-folds reduction respectively. We attribute this effect to the presence of the new DA-LA conjugates that facilitate the aggregation, probably due to an increase in the total associative hydrophobicity of the system, which results in stronger attractive forces between DA and DA-LA molecules.

To test whether the observed effect on CAC can be attributed to reaction products of DA-LA or to other molecules in the mixtures, i.e., LA monomers or LA oligomers, we performed control experiments. To that end, we measured the CAC of DA at pH 6.8 in the presence of LA monomers or oligomers. When LA monomers were introduced at concentrations of 100 mM and 200 mM, the CAC only slightly decreased from 10mM to about 9.8 mM and 9.3 mM respectively (Figure 5 and Figures S201-S202). The presence of LA oligomers, by contrast, had no significant effect on DA's CAC (Figure 5 and Figures S203-S204). Several factors have been found to promote DA aggregation, including salinity enhancement and additions of lipidic components or other amphiphiles.[22,58] The effect of salts, for instance, is the result of the significant increase in water polarity, essentially turning the amphipathic molecules more hydrophobic .[59] This effect was also observed for LA monomers, albeit to a much lesser extent. The effect of DA-LA conjugates was mechanistically related to the hydrophobic interactions, as was also demonstrated in the case of n-decanol, glycerol mono decanoate, and decylamine, for which their presence led to a reduction of the CVC of DA by up to 10-fold.[22,23] Notably, for the reaction products of DA:LA at a 1:4 molar ratio and pH 6.8, both vesicles and micelles were observed. Therefore, the determined CAC might be attributed to either the micelles or the vesicles. Nonetheless, the concentration is significantly lower than that of DA control samples prepared in the presence and absence of LA monomers or oligomers, highlighting the superior assembly propensity of DA-LA conjugates.

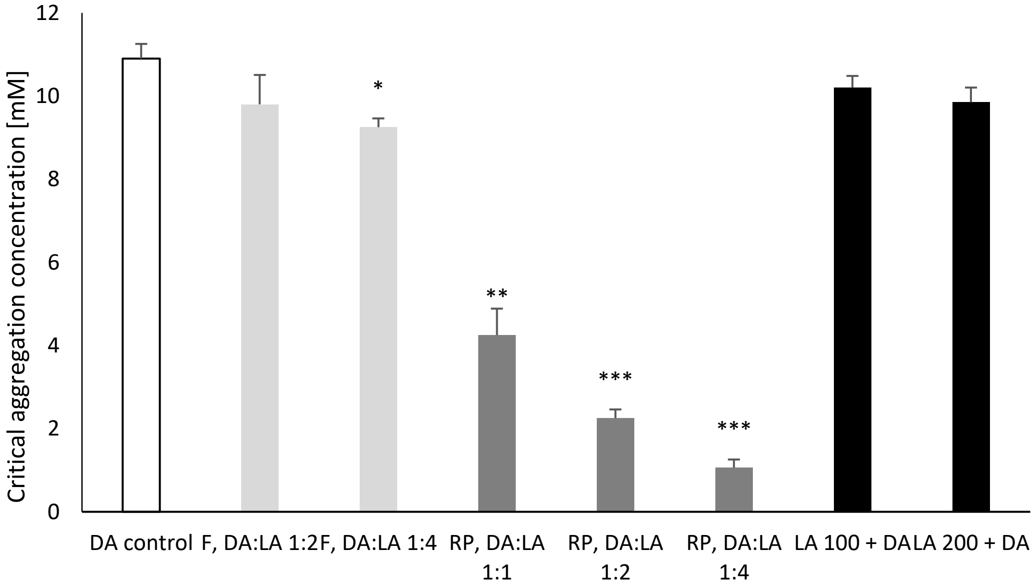

Figure 5. Critical aggregation concentration (CAC) of DA obtained for DA-LA fresh monomers (F, light grey columns), DA-LA reaction products (RP, dark grey columns), and for DA in the presence of LA oligomers (black columns). The oligomerization of DA into DA-(LA)$_n$ conjugates resulted in the reduction of DA CAC at pH 6.8 by up to 10-fold. The presence of either LA monomers or LA oligomers had only a minor effect on the CAC of DA.

Differential hydrolysis of LA-DA reaction products.

In the context of origins of life, except for self-assembly and structural properties of prebiotic molecules, which are highly important for compartmentalization, the hydrolysis of such molecules is also crucial. The survival of certain molecules is closely related to their capability to avoid hydrolysis in aqueous environments.[41] As indicated by LC-MS measurements, the products of the reaction between DA and LA comprised two different types of oligomers: LA homoesters and DA-LA heteroesters, both of which contain hydrolysable ester bonds. Therefore, we sought to study the degradation of the esterified products, which can occur both via regular hydrolysis or through a back-biting mechanism.[60] To that end, we focused on the reaction product of DA:LA at 1:4 molar and studied the degradation rates of LA homoesters and DA-LA heteroesters at pH 6.8 and 40 °C for a period of 72 hours. The most prominent observation was the differential degradation rates of LA homoesters compared to DA-LA heteroesters. At this timescale, LA homoesters were gradually hydrolyzed within this period, and, after 8 hours, only trace amounts of LA pentamer and tetramer were observed. The shortest oligomers, LA dimer and LA trimer, were detected even after 72 hours. As opposed to the homoesters, LA-DA heteroesters of up to LA_5DA were detected even after 72 hours (Figure 6 and Figures S205-S206). It is worth noting that over the course of the hydrolysis experiment, the pH levels remained constant. The hydrolysis rate of the products was further determined in terms of product degradation by monitoring the changes in the peak area of each product. Indeed, LA monomers, dimers, and trimers accumulated over the initial incubation period at the expense of the longer homooligomers and heterooligomers (Figure 6A). At the end of the experiment, LA monomers had doubled in terms of peak area and LA dimers had increased by ~1.5-fold compared to the beginning of the reaction (Figure 6B-C). In the case of LA-DA heteroesters, LA_1DA and LA_2DA accumulated 1.3-fold over the incubation period at the expense of the longer LA-DA oligomers (Figure 6A,C). Yet the levels of DA were slightly decreased, probably due to minor evaporation over the course of the reaction (Figure 6B).

From the perspective of LA oligomers, when comparing the persistence of those that were not conjugated to DA to those that were conjugated to DA, one can clearly see the enhanced chemical stability of the oligomers that were conjugated to DA over the ones that were not. For instance, 30% of LA trimers that were not conjugated to DA were hydrolyzed after 72 hours at 40 °C, while the corresponding ones that were conjugated to DA were practically not hydrolyzed over the course of the experiment (Figure 6D). In the case of the longer oligomers, the resistance to hydrolysis was even more pronounced when the oligomers were conjugated to DA: a reduction of 82% after 8 hours at 40 °C in the peak area of LA pentamers that were not conjugated to DA was observed, compared to only 13% for the DA-conjugated ones (Figure 6E-F). The non-conjugated LA pentamers were completely hydrolyzed after 72 hours, while the DA-conjugated pentamers were only partially hydrolyzed, with a reduction of 35%. The faster hydrolysis rate of homoesters compared to heteroesters was also observed across various pH levels (5.5, 6.8, or 8.0) and temperatures (room temperature (RT), 40 °C, or 60 °C) (Figures S207-S218). As expected, the hydrolysis rate of both types of products was temperature- and pH-dependent.

The immense protection against hydrolysis can be attributed to structure formation. Upon structure formation, the accessibility of the ester groups to hydrolysis via water molecules or to back-biting is significantly hindered. Medium chain fatty acids and their ester derivatives are known to form various structures.[61] A study by Bonfio *et al.* achieved accumulation of medium-chain acylglycerol-phosphates over short-chain acylglycerol-phosphate through iterative acylation-hydrolysis cycles. The accumulation was accompanied by vesicle formation. The authors ascribed this effect to the selective hydrolysis of the shorter-chain acylglycerol-phosphate due to their lack of self-assembly capability. Regardless of the particular nature of the amphiphile or the specific nature of the assembly, the hydrolysis rate is highly dependent on the concentration of the amphiphiles and on the presence of structures. Typically hydrolysis rates are hindered upon assembly, even though the reverse phenomenon has also been observed.[62-64] In addition, studies have demonstrated that sucrose esters tend to hydrolyze to a greater extent under acidic conditions below their critical micelles concentration (CMC).[65] Ethoxylated fatty esters hydrolysis under basic conditions was also hindered due to the presence of micelles compared to the non-aggregated surfactants.[66] This hydrolysis inhibition manifested in different kinetics of the hydrolysis; above the CMC of the tested ethoxylated fatty esters, hydrolysis profiles fit pseudo zero-order reaction while below the CMC first-order kinetics was observed. Remarkably, the protective effect of self-assembly is observed in that study even under basic conditions, which is remarkable given that ester bonds hydrolyze much faster under basic conditions.[67] The authors primarily attributed this to the fact that the ester bond is not accessible to the hydroxide ions as a result of micelle formation. Other physicochemical characteristics, such as polarity of the structure's surface and its charge, significantly affect the hydrolysis rate as well.

The selective hydrolysis of LA homoesters as opposed to the hydrolysis of LA-DA heteroesters suggests that the LA homoesters formed in the dry reaction in the presence of DA are not capable of self-assembly under tested conditions (Figure S195). Indeed, these esters were found to be shorter than those obtained in the absence of DA, which can affect their aggregation properties. It is worth noting that even if LA homoesters do not form structures by themselves under the tested conditions, co-aggregation with DA and its products is theoretically possible. However, based on our results, such co-aggregation is very unlikely due to the rapid hydrolysis of the homoesters. For instance, the hydrolysis of ethyl benzoate and several aliphatic esters was significantly inhibited in the presence of anionic, cationic, and nonionic surfactants above their CMC in a concentration-dependent manner.[68] The authors ascribed this effect to the presence of esters-micelles complexes. The partitioning of the esters in the bulk and in the micellar phases resulted in overall inhibition of hydrolysis rates.

We further examined the hydrolysis of LA homoesters obtained by the dry reaction of LA at 85°C in the absence of DA. As mentioned, in the absence of DA, LA oligomerized to a greater extent, forming longer homoesters. These products form aggregates at pH 6.8, as indicated by microscopy (Figure S195). Upon incubation at RT and pH 6.8 for up to 4 days, LA homoesters of medium chain length hydrolyzed while the longest ones were still detected and exhibited lower degradation rates (Figures S219-S222). This result underlines the crucial protective role of self-assembly against degradation in water, which is a universal phenomenon and is not limited to a certain type of self-assembly.[41]

Novel chemical approach for the synthesis of amphiphile mixtures.

Amphiphiles based on HA derivatives, especially the ones obtained by the condensation of fatty acids and HAs, have been known for years and used for several applications in the food and pharma industries.[69,70] The current synthesis strategies of such amphiphiles involve either one-step or two-step reactions.[70,71] In one-step reactions, lactic acid, fatty acid, and sodium carbonate are reacted together, while the two-step reactions involve consecutive polymerization and esterification. These surfactants are considered environmentally friendly and biodegradable. The current derivatives of HA amphiphiles are mostly fatty acyl lactylates, which are mixtures of molecules with various lactic acid polymerization degrees.[52,72] Our simple prebiotic, green synthesis was found to be highly reproducible and resulted in a mixture of both homoesters of the HA and heteroesters of the DA-HA conjugates that exhibit unique properties and can be used for multiple applications. The differential hydrolytic rates of the homo- and hetero- esters can be used for the selective release of drugs based on their affinity to either type of oligomer.

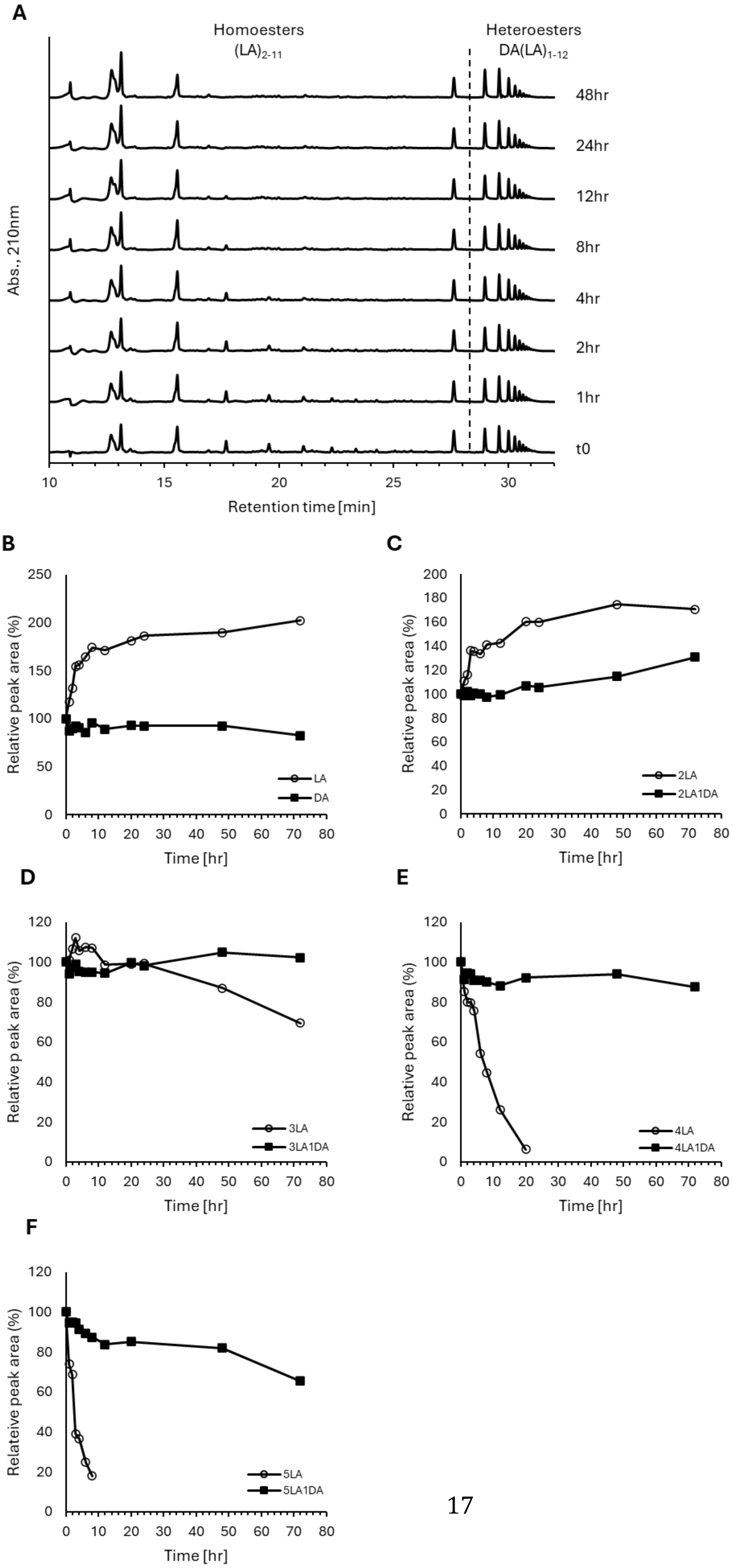

Figure 6. DA-LA heteroesters exhibit greater persistence than LA homoesters. Chromatograms obtained for the DA:LA reaction product at 1:4 molar ratio. The reaction product was rehydrated in a phosphate buffer (50 mM) at pH 6.8 and stored at 40 °C for a period of 72 hours during which samples were withdrawn and analyzed via HPLC (A). Changes in the peak area of LA (empty circles) and DA (filled squares) monomers over the course of the incubation are shown (B). LA accumulated over the incubation period while DA levels decreased slightly. Changes in the peak area of LA dimers that were not covalently bound to DA (empty circles) and LA dimers covalently bound to DA (filled squares) are shown (C). Changes in the peak area of LA trimers that were not covalently bound to DA (empty circles) and LA trimers covalently bound to DA (filled squares) are shown (D). Changes in the peak area of LA tetramers that were not covalently bound to DA (empty circles) and LA tetramers covalently bound to DA (filled squares) are shown (E). Changes in the peak area of LA pentamers that were not covalently bound to DA (empty circles) and LA pentamers covalently bound to DA (filled squares) are shown (F). LA dimers accumulated over the course of the reaction regardless of the conjugation to DA. By contrast, longer LA oligomers were more persistent when covalently bound to DA. For longer oligomers the protective effect of the conjugation is more pronounced, as indicated in panels D-F.

The universality of mutualism between hydroxy acids and lipids.

The process of chemical evolution has led to the emergence of the four fundamental, well-organized components of life: proteins, carbohydrates, nucleic acids, and lipids. It is plausible that throughout this evolutionary process, the individual pathways leading to the formation of these major biomolecular classes have occasionally converged, giving rise to symbiotic coevolution. In such cases, mutual interactions between different evolving molecular species may have contributed to their evolutionary trajectory. An example of this is the interaction of DA and LA, which exhibited characteristics of symbiotic coevolution where both molecular species benefited; LA oligomers gained greater hydrolytic stability when were conjugated to DA, and DA molecules formed vesicles more readily and at lower concentrations when linked to LA oligomers.

To assess whether this mutualistic effect is generalizable, we tested additional lipid-hydroxy acid systems. Specifically, we performed hydrolysis assays and determination of the CAC for mixtures of either octanoic acid and dodecanoic acid with LA, DA with PLA, and a ternary mixture of DA with both LA and GA (Supplementary Methods). Indeed, the hydrolysis assays confirmed the positive effect of fatty acid conjugation: all tested oligomers showed enhanced hydrolytic stability when covalently linked to fatty acids (Figures S223-S230). In turn, the conjugated HA oligomers facilitated the aggregation of the lipids as indicated by the merocyanine assay. For instance, the CAC of octanoic acid, decanoic acid, and dodecanoic acid decreased by approximately tenfold upon conjugation with LA oligomers (Figures S231-S238). These results demonstrate that the mutualistic effect between DA and LA is generalizable to various lipid-hydroxy acid systems and further support the plausibility of symbiotic coevolution of different molecular species.

In the past decanoic acid (DA) and hydroxy acids (HAs) have been investigated separately in the context of origins of life as a protocell model amphiphile and as a protopeptide model, respectively. In this work we studied the coevolution of these two different building blocks focusing on the interplay between polymerization, hydrolysis, and compartmentalization. Through simple drying reactions, we were able to generate novel amphiphiles derived from DA-HA ester conjugates that readily self-assemble in aqueous solutions. We focused our investigation on drying reactions between DA and lactic acid (LA), which produced a mixture of both homoesters and heteroesters. The structural characteristics of DA assemblies were positively affected by the presence of LA-DA heteroesters, lowering the critical assembly concentration of the amphiphile and facilitating the formation of both vesicles and micelles. In a mutualistic manner, the LA oligomers that were conjugated to DA exhibited slower degradation rates than the corresponding LA homoesters. Further studies with additional lipid-hydroxy acid systems have shown that the mutualistic effect between DA and LA is generalizable. Our results shed light on the crucial role of interdependent assembly in the process of chemical evolution, demonstrating that oligomerization and compartmentalization could have evolved together in a synergistic fashion.

Methods

Single-step dry reactions. Binary mixtures of decanoic acid (DA) and hydroxy acids (HAs) at 1:1, 1:2, and 1:4 molar ratios were prepared in 7mL scintillation vials. DA's amount was fixed at 200 µmol and HAs' amount was adjusted accordingly. All components were weighed except for lactic acid which was added volumetrically. The mixtures were placed at 85 °C for seven days. Samples of either DA (200 µmol) alone or hydroxy acids (400 µmol) alone were prepared as control. An aliquot of 1M HCl (1 µmol) was added to the DA control. All samples were prepared in triplicates. Similar procedure was carried out for the other mixtures of fatty acids (FAs) and HAs.

Samples rehydration and structure reconstitution. For structural characterization, crude reaction products were rehydrated in water, concentrated phosphate monobasic solution (1.0 M), and NaOH solution (1.0 M). Samples were vigorously mixed, and their pH was adjusted to 6.8 using NaOH. DA and HAs concentration was 50 mM and 50 mM-200 mM, respectively, referring to initial amounts prior to the reaction. The final buffer concentration was 50 mM. The samples were kept at room temperature for 16-24 hr prior to characterization. All samples were prepared in triplicates.

High-Performance Liquid Chromatography / LC-MS. HPLC analyses were conducted using an Agilent 1260 quaternary pump and autosampler (Agilent Technologies, Santa Clara, CA, USA) with a DAD UV-vis detector at 210nm and 259nm. LC-MS data were collected using an Agilent G6135C single quadrupole mass spectrometer with a capillary voltage of 4.0 kV and a source fragmentation voltage of 70 V. Scan range: 50-1500 m/z. Chromatographic separation was achieved using InfinityLab Poroshell 120 EC-C18 column (150 x 3.0 mm, 2.7 µm, with a SecurityGuard^{TM} C18 4x2.0mm), at a constant 0.3 mL/min flow rate. Column cell temperature was maintained at 20 °C. Gradient elution was carried out using (A) 0.1% formic acid in water and (B) acetonitrile as follow: 5min 100% A, 20min ramp to 20% A, 10min 100% B. Further details on chromatographic methods are given in the SI.

Preparation of FA standard solutions for HPLC analyses. Stock solutions of FA were prepared by dissolving FA in acetonitrile (ACN) in volumetric flasks. Calibration standards of concentration ranging between 1 mM to 8 mM were prepared by diluting FA stock solution in ACN:water 50:50.

Preparation of samples for HPLC analyses. The samples obtained from the dry reactions were dissolved in ACN and sonicated to allow the complete extraction of the analytes. All samples were completely solubilized in ACN except for GA samples which were only partially solubilized. Samples were further diluted in ACN:water 50:50 to reach a final concentration of

5 mM FA, referring to initial amounts prior to the reaction. The consumption of DA was calculated using the calibration curve.

ATR-FTIR measurements. Attenuated total reflectance Fourier transform infrared measurements were carried out on a Jasco (Tokyo, Japan) FT/IR-4X1 Spectrometer. Prior to measurement, 50 µL of 100 mM samples solubilized in acetonitrile were placed on aluminum foil and allowed to dry under ambient conditions. The aluminum foil was then placed in an Attenuated Total Reflectance (ATR) sample chamber for analysis of the dried sample. Spectra were signal averaged (60 scans per spectrum) and background-subtracted and ranged from 400 to 4000 cm^{-1}. Spectra were analyzed using Excel software.

NMR Spectroscopy. ^1H-NMR spectra were recorded on a 500 MHz Neo spectrometer. Reaction products or fresh monomers were dispersed in chloroform-D_3 and sonicated for 1 min in an ice bath. In the case of glycolic acid and malic acid, fresh monomers and the HA controls were also dispersed in D_2O. All data were plotted and processed using the TopSpin software.

Microscopy imaging. 100 µL of reconstituted samples were mixed with rhodamine 6G solution (which was prepared in ethanol). Final dye concentration was 1 mM. Images were conducted utilizing a ECHO Revolve microscope (ECHO, San Diego CA), equipped with a 8MP CMOS Color camera, with a magnification of X60 Olympus® air objective. FITC filter (EX: 470/40, EM: 525/50, DM: 495) was used for both fluorescent and bright field measurements.

Cryogenic-Transmission Electron Microscopy (Cryo-TEM). FEI Tecnai 12 G2 TWIN TEM Operated at 120 kV and equipped with a Gatan Model 626 Cold Stage was used. The Images were recorded by a 4 k × 4 k FEI Eagle CCD Camera in Low Dose Mode. TIA (Tecnai Imaging and Analysis) software was used to record the images. Prior to measurements, 3 µL samples were applied onto a glow-discharged TEM grid (300-mesh Cu grid) coated with a holey carbon film (Lacey substrate, Ted Pella, Ltd., 4595 Mountain Lakes Blvd., Redding, CA, USA). The excess liquid was blotted for 2 seconds, and the specimens were vitrified by a rapid plunging into liquid ethane precooled with liquid nitrogen using Vitrobot Mark IV (FEI).

Turbidity measurements. Turbidity measurements were carried out on a Synergy H1 plate reader (BioTek Instruments, VT, USA). 200 µL samples were placed in 96-wells plate in technical duplicates. Spectra were recorded between 400 nm to 800 nm. Turbidity was reported as the absorbed light at 400nm.

Critical aggregation concentration (CAC) determination. The critical aggregation concentration of DA and other fatty acids (FAs) in fresh controls and reaction products was determined using the Merocyanine 540 assay. to that end, dilution lines were prepared by diluting stocks of fresh monomers or reaction products (see sample rehydration) with phosphate buffer and pH was adjusted as required. The dilution lines were constructed to cover a range of FA concentration which are below and above the CAC. The resulting dilutions were mixed with Merocyanine 540 stock of 1mg/mL, resulting in final Merocyanine 540 concentration of 20µg/mL. 150µL sample were placed in 96-wells black plate. Spectra were recorded on a Synergy H1 plate reader (BioTek Instruments, VT, USA) between 400 nm to 620 nm. The ratio between the absorption at 570 nm and 530 nm was calculated and plotted against FA concentration. The point at which the ratio increases significantly was considered as the CAC. The determined values were extracted from the intersection between the linear fitting lines at the two first regions of the curves.

Hydrolysis and degradation experiments. The hydrolysis and degradation profile of the dried products obtained in the drying reactions was evaluated for various reaction products. Crude reaction products were rehydrated in water and with either 1M solutions of tris, phosphate monobasic, or citric acid, and the pH of the samples was further adjusted to 8.0, 6.8, or 5.5, respectively. The resulting rehydrated samples were dispensed into aliquots in 1.5 mL microtubes. Each sample was withdrawn at different time points. Samples were stored at various temperatures (RT, 40°C or 60°C) and withdrawn at different time points. All withdrawn samples stored at -80 °C until being analyzed by HPLC/ LC-MS. Prior to HPLC analyses, the pH of each sample was roughly measured using a pH Indicator Strip, universal Specification (0 - 14.0) (Millipore, Merck). For HPLC analyses, samples were diluted four to ten times fold . To confirm that no degradation occurred during the analysis itself, representative samples were injected several times during the course of the analysis.

Control samples of LA reaction products using the initial amount of either 400 µmol or 800 µmol were tested for hydrolysis as well. The dry reaction products were rehydrated in water and phosphate buffer and the pH was adjusted to 6.8. The final concentration of LA was either 100 mM or 200 mM, referring to initial amounts prior to the reaction. The rehydrated products were stored at RT and samples of 800 µL were withdrawn immediately after preparation and after 12hr and 4 days. The withdrawn samples were treated as described above.

To monitor the degradation rate of the products, the area of each product was integrated by OpenLab software using Chemstation integrator. Every peak area obtained at each time point was normalized to t0 and the relative change was plotted over time.

Statistical significance. Student's t-test was used to determine statistical significance.

Data availability

All the data supporting the findings of this study are available within the main text and its Supplementary Information.

References

1 Monnard, P.-A. & Walde, P. Current Ideas about Prebiological Compartmentalization. *Life* **5**, 1239-1263 (2015). https://doi.org/10.3390/life5021239

2 Guo, W. *et al.* Non-associative phase separation in an evaporating droplet as a model for prebiotic compartmentalization. *Nature Communications* **12** (2021). https://doi.org/10.1038/s41467-021-23410-7

3 Mizuuchi, R. & Ichihashi, N. Primitive Compartmentalization for the Sustainable Replication of Genetic Molecules. *Life* **11**, 191 (2021). https://doi.org/10.3390/life11030191

4 Lombard, J., López-García, P. & Moreira, D. The early evolution of lipid membranes and the three domains of life. *Nature Reviews Microbiology* **10**, 507-515 (2012). https://doi.org/10.1038/nrmicro2815

5 Santos, T. C. B. & Futerman, A. H. The fats of the matter: Lipids in prebiotic chemistry and in origin of life studies. *Progress in Lipid Research* **92**, 101253 (2023). https://doi.org/10.1016/j.plipres.2023.101253

6 Morigaki, K. & Walde, P. Fatty acid vesicles. *Curr. Opin. Coll. Interf. Sci.* **12**, 75-80 (2007).

7 Proskurowski, G. *et al.* Abiogenic hydrocarbon production at lost city hydrothermal field. *Science* **319**, 604-607 (2008). https://doi.org/10.1126/science.1151194

8 McCollom, T. M. & Simoneit, B. R. Abiotic formation of hydrocarbons and oxygenated compounds during thermal decomposition of iron oxalate. *Origins of Life and Evolution of the Biosphere* **29**, 167-186 (1999).

9 Lawless, J. G. & Yuen, G. U. Quantification of monocarboxylic acids in the Murchison carbonaceous meteorite. *Nature* **282**, 396-398 (1979). https://doi.org/10.1038/282396a0

10 Schmitt-Kopplin, P. *et al.* High molecular diversity of extraterrestrial organic matter in Murchison meteorite revealed 40 years after its fall. *Proceedings of the National Academy of Sciences* **107**, 2763-2768 (2010).

11 Fiore, M. *et al.* Synthesis of Phospholipids Under Plausible Prebiotic Conditions and Analogies with Phospholipid Biochemistry for Origin of Life Studies. *Astrobiology* **22**, 598-627 (2022). https://doi.org/10.1089/ast.2021.0059

12 Bonfio, C. *et al.* Length-Selective Synthesis of Acylglycerol-Phosphates through Energy-Dissipative Cycling. *Journal of the American Chemical Society* **141**, 3934-3939 (2019). https://doi.org/10.1021/jacs.8b12331

13 Liu, L. *et al.* Enzyme-free synthesis of natural phospholipids in water. *Nature Chemistry* **12**, 1029-1034 (2020). https://doi.org/10.1038/s41557-020-00559-0

14 Powner, M. & Fernández-García, C. Selective Acylation of Nucleosides, Nucleotides, and Glycerol-3-phosphocholine in Water. *Synlett* **28**, 78-83 (2016). https://doi.org/10.1055/s-0036-1588626

15 Aleksandrova, M., Rahmatova, F., Russell, D. A. & Bonfio, C. Ring Opening of Glycerol Cyclic Phosphates Leads to a Diverse Array of Potentially Prebiotic Phospholipids. *Journal of the American Chemical Society* **145**, 25614-25620 (2023). https://doi.org/10.1021/jacs.3c07319

16 Deamer, D. The Role of Lipid Membranes in Life's Origin. *Life* **7**, 5 (2017). https://doi.org/10.3390/life7010005

17 Monnard, P.-A. & Deamer, D. W. 133-151 (Elsevier, 2003).

18 Apel, C. L., Deamer, D. W. & Mautner, M. N. Self-assembled vesicles of monocarboxylic acids and alcohols: conditions for stability and for the encapsulation of biopolymers. *Biochimica et Biophysica Acta (BBA) - Biomembranes* **1559**, 1-9 (2002). https://doi.org/10.1016/s0005-2736(01)00400-x

19 Namani, T. & Walde, P. From Decanoate Micelles to Decanoic Acid/Dodecylbenzenesulfonate Vesicles. *Langmuir* **21**, 6210-6219 (2005). https://doi.org/10.1021/la047028z

20 Namani, T., Ishikawa, T., Morigaki, K. & Walde, P. Vesicles from docosahexaenoic acid. *Colloids and Surfaces B: Biointerfaces* **54**, 118-123 (2007).

21 Yamagami, R., Sieg, J. P. & Bevilacqua, P. C. Functional Roles of Chelated Magnesium Ions in RNA Folding and Function. *Biochemistry* **60**, 2374-2386 (2021). https://doi.org/10.1021/acs.biochem.1c00012

22 Maurer, S. E., Deamer, D. W., Boncella, J. M. & Monnard, P.-A. Chemical evolution of amphiphiles: glycerol monoacyl derivatives stabilize plausible prebiotic membranes. *Astrobiology* **9**, 979-987 (2009).

23 Maurer, S. E. *et al.* Vesicle self-assembly of monoalkyl amphiphiles under the effects of high ionic strength, extreme pH, and high temperature environments. *Langmuir* **34**, 15560-15568 (2018).

24 Black, R. A. *et al.* Nucleobases bind to and stabilize aggregates of a prebiotic amphiphile, providing a viable mechanism for the emergence of protocells. *Proceedings of the National Academy of Sciences* **110**, 13272-13276 (2013).

25 Cornell, C. E. *et al.* Prebiotic amino acids bind to and stabilize prebiotic fatty acid membranes. *Proceedings of the National Academy of Sciences* **116**, 17239-17244 (2019).

26 Cohen, Z. R., Ramsay, A., Cornell, C. E., Black, R. A. & Keller, S. L. Amino Acids Bind to and Influence the Structure of Fatty Acid Vesicles. *Biophysical Journal* **116**, 509a-510a (2019). https://doi.org/10.1016/j.bpj.2018.11.2748

27 Black, R., Cohen, Z., Todd, Z., Maibaum, L. & Catling, D. *Stabilization of prebiotic vesicles by peptides depends on sequence and chirality* (Research Square Platform LLC, 2023).

28 Hirai, A. *et al.* Effects of l-arginine on aggregates of fatty-acid/potassium soap in the aqueous media. *Colloid and Polymer Science* **284**, 520-528 (2006). https://doi.org/10.1007/s00396-005-1423-1

29 Bomba, R., Kwiatkowski, W., Sánchez-Ferrer, A., Riek, R. & Greenwald, J. Cooperative Induction of Ordered Peptide and Fatty Acid Aggregates. *Biophys J* **115**, 2336-2347 (2018). https://doi.org/10.1016/j.bpj.2018.10.031

30 Mandal, R. *et al.* Self-assembled prebiotic amphiphile-mixture exhibits tunable catalytic properties. *Organic & Biomolecular Chemistry* **21**, 4473-4481 (2023). https://doi.org/10.1039/d3ob00606a

31 Namani, T. *et al.* Novel Chimeric Amino Acid-Fatty Alcohol Ester Amphiphiles Self-Assemble into Stable Primitive Membranes in Diverse Geological Settings. *Astrobiology* **23**, 327-343 (2023). https://doi.org/10.1089/ast.2022.0056

32 Joshi, M. P., Sawant, A. A. & Rajamani, S. Spontaneous emergence of membrane-forming protoamphiphiles from a lipid–amino acid mixture under wet–dry cycles. *Chemical Science* **12**, 2970-2978 (2021). https://doi.org/10.1039/d0sc05650b

33 McCollom, T. M., Ritter, G. & Simoneit, B. R. Lipid synthesis under hydrothermal conditions by Fischer-Tropsch-type reactions. *Origins of Life and Evolution of the Biosphere* **29**, 153-166 (1999).

34 Aponte, J. C. *et al.* Analysis of amino acids, hydroxy acids, and amines in CR chondrites. *Meteoritics & Planetary Science* **55**, 2422-2439 (2020).

35 Forsythe, J. G. *et al.* Ester-Mediated Amide Bond Formation Driven by Wet–Dry Cycles: A Possible Path to Polypeptides on the Prebiotic Earth. *Angewandte Chemie International Edition* **54**, 9871-9875 (2015). https://doi.org/10.1002/anie.201503792

36 Frenkel-Pinter, M. *et al.* Differential Oligomerization of Alpha versus Beta Amino Acids and Hydroxy Acids in Abiotic Proto-Peptide Synthesis Reactions. *Life* **12**, 265 (2022). https://doi.org/10.3390/life12020265

37 Frenkel-Pinter, M. *et al.* Selective incorporation of proteinaceous over nonproteinaceous cationic amino acids in model prebiotic oligomerization reactions. *Proceedings of the National Academy of Sciences* **116**, 16338-16346 (2019). https://doi.org/10.1073/pnas.1904849116

38 Jia, T. Z. *et al.* Membraneless polyester microdroplets as primordial compartments at the origins of life. *Proceedings of the National Academy of Sciences* **116**, 15830-15835 (2019).

39 Afrin, R. *et al.* The Effects of Dehydration Temperature and Monomer Chirality on Primitive Polyester Synthesis and Microdroplet Assembly. *Macromolecular Chemistry and Physics* **223**, 2200235 (2022). https://doi.org/10.1002/macp.202200235

40 Chen, C. *et al.* Spectroscopic and Biophysical Methods to Determine Differential Salt-Uptake by Primitive Membraneless Polyester Microdroplets. *Small Methods* **7** (2023). https://doi.org/10.1002/smtd.202300119

41 Edri, R., Fisher, S., Menor-Salvan, C., Williams, L. D. & Frenkel-Pinter, M. Assembly-driven protection from hydrolysis as key selective force during chemical evolution. *FEBS letters* **597**, 2879-2896 (2023).

42 Runnels, C. M. *et al.* Folding, Assembly, and Persistence: The Essential Nature and Origins of Biopolymers. *Journal of Molecular Evolution* **86**, 598-610 (2018). https://doi.org/10.1007/s00239-018-9876-2

43 Sepulveda, R. V. *et al.* Insights into Early Steps of Decanoic Acid Self-Assemblies under Prebiotic Temperatures Using Molecular Dynamics Simulations. *Membranes* **13**, 469 (2023). https://doi.org/10.3390/membranes13050469

44 Cistola, D. P., Hamilton, J. A., Jackson, D. & Small, D. M. Ionization and phase behavior of fatty acids in water: application of the Gibbs phase rule. *Biochemistry* **27**, 1881-1888 (1988).

45 Lowe, L. A. *et al.* Subtle changes in pH affect the packing and robustness of fatty acid bilayers. *Soft Matter* **18**, 3498-3504 (2022). https://doi.org/10.1039/d2sm00272h

46 Ashkenasy, G., Hermans, T. M., Otto, S. & Taylor, A. F. Systems chemistry. *Chemical Society Reviews* **46**, 2543-2554 (2017). https://doi.org/10.1039/c7cs00117g

47 Mattia, E. & Otto, S. Supramolecular systems chemistry. *Nature Nanotechnology* **10**, 111-119 (2015). https://doi.org/10.1038/nnano.2014.337

48 Ruiz-Mirazo, K., Briones, C. & de la Escosura, A. Prebiotic systems chemistry: new perspectives for the origins of life. *Chem Rev* **114**, 285-366 (2014). https://doi.org/10.1021/cr2004844

49 Kwiatkowski, W. *et al.* Prebiotic Peptide Synthesis and Spontaneous Amyloid Formation Inside a Proto-Cellular Compartment. *Angewandte Chemie* **60**, 5561-5568 (2021). https://doi.org/10.1002/anie.202015352

50 Lancet, D., Zidovetzki, R. & Markovitch, O. Systems protobiology: origin of life in lipid catalytic networks. *J R Soc Interface* **15** (2018). https://doi.org/10.1098/rsif.2018.0159

51 Chong, C. & Colbow, K. Light scattering and turbidity measurements on lipid vesicles. *Biochimica et Biophysica Acta (BBA)-Biomembranes* **436**, 260-282 (1976).

52 Fan, J. *et al.* Synthesis and properties of sodium fatty acyl lactylates. *Colloids and Surfaces A: Physicochemical and Engineering Aspects* **653**, 129946 (2022). https://doi.org/10.1016/j.colsurfa.2022.129946

53 Zhu, T. F. & Szostak, J. W. Coupled growth and division of model protocell membranes. *Journal of the American Chemical Society* **131**, 5705-5713 (2009).

54 Budin, I., Debnath, A. & Szostak, J. W. Concentration-Driven Growth of Model Protocell Membranes. *Journal of the American Chemical Society* **134**, 20812-20819 (2012). https://doi.org/10.1021/ja310382d

55 Kahana, A. & Lancet, D. Self-reproducing catalytic micelles as nanoscopic protocell precursors. *Nature Reviews Chemistry* **5**, 870-878 (2021). https://doi.org/10.1038/s41570-021-00329-7

56 Kara, H., Kaya, M. & Onganer, Y. Molecular aggregates of merocyanine 540 with different surfactant systems. *Journal of Molecular Liquids* **412**, 125831 (2024). https://doi.org/10.1016/j.molliq.2024.125831

57 Bernik, D. & Disalvo, E. Determination of the dimerization constant of merocyanine 540 at the membrane interface of lipid vesicles in the gel state. *Chemistry and physics of lipids* **82**, 111-123 (1996).

58 Maurer, S. E. & Nguyen, G. Prebiotic Vesicle Formation and the Necessity of Salts. *Origins of Life and Evolution of Biospheres* **46**, 215-222 (2016). https://doi.org/10.1007/s11084-015-9476-8
59 Kahlweit, M., Strey, R., Schomaecker, R. & Haase, D. General patterns of the phase behavior of mixtures of water, nonpolar solvents, amphiphiles, and electrolytes. 2. *Langmuir* **5**, 305-315 (1989). https://doi.org/10.1021/la00086a002
60 C, M. *et al.* Water-Based Dynamic Depsipeptide Chemistry: Building Block Recycling and Oligomer Distribution Control Using Hydration–Dehydration Cycles. *JACS Au* **2**, 1395-1404 (2022). https://doi.org/10.1021/jacsau.2c00087
61 Kulkarni, C. V. Lipid crystallization: from self-assembly to hierarchical and biological ordering. *Nanoscale* **4**, 5779 (2012). https://doi.org/10.1039/c2nr31465g
62 Abe, Y., Watanabe, H. & Fujiwara, M. Micellar Effects on the Hydrolysis Reaction of an Anionic Surfactant in Aqueous Solution. *Langmuir* **34**, 13979-13992 (2018). https://doi.org/10.1021/acs.langmuir.8b03451
63 Lundberg, D., Stjerndahl, M. & Holmberg, K. Ester-based surfactants: Are they stable enough? *Journal of Surfactants and Detergents* **26**, 229-236 (2023). https://doi.org/10.1002/jsde.12628
64 Bayissa, L. D., Ohmae, Y. & Hojo, M. Influences of Micelle Formation and Added Salts on the Hydrolysis Reaction Rate of <i>p</i>-Nitrophenyl Benzoate in Aqueous Buffered Media. *International Journal of Chemical Kinetics* **49**, 71-82 (2017). https://doi.org/10.1002/kin.21052
65 Okumura, H., Kitazawa, N., Wada, S. & Hotta, H. Stability of sucrose fatty acid esters under acidic and basic conditions. *Journal of oleo science* **60**, 313-320 (2011).
66 Stjerndahl, M. & Holmberg, K. Synthesis and chemical hydrolysis of surface-active esters. *Journal of Surfactants and Detergents* **6**, 311-318 (2003). https://doi.org/10.1007/s11743-003-0275-0
67 Sun, Y., Frenkel-Pinter, M., Liotta, C. L. & Grover, M. A. The pH dependent mechanisms of non-enzymatic peptide bond cleavage reactions. *Physical Chemistry Chemical Physics* **22**, 107-113 (2020). https://doi.org/10.1039/c9cp05240b
68 Xiancheng, Z. *et al.* The effect of cationic, anionic, and nonionic surfactant micelles on the alkaline hydrolysis of esters. *Journal of Dispersion Science and Technology* **16**, 531-541 (1995). https://doi.org/10.1080/01932699508943705
69 Additives, E. P. o. F. *et al.* Re-evaluation of acetic acid, lactic acid, citric acid, tartaric acid, mono-and diacetyltartaric acid, mixed acetic and tartaric acid esters of mono-and diglycerides of fatty acids (E 472a-f) as food additives. *EFSA Journal* **18**, e06032 (2020).
70 Zielinski, R. Synthesis and composition of food-grade emulsifiers. *Food emulsifiers and their applications*, 11-38 (1997).
71 Xuexin, Y. Preparation and Application of Stearyl Sodium Lactate. *Advance Journal of Food Science and Technology* **10**, 437-442 (2016). https://doi.org/10.19026/ajfst.10.2156
72 Meshram, P. D. & Jadhav, S. R. Preparation and properties of lactic acid-based modified carboxylic surfactant. *J Surf Sci Technol* **28**, 149-161 (2012).

Acknowledgments

We thank Eliav Marland and Or Cohen for fruitful discussions. This research was supported by the Azrieli Foundation Early Career Faculty Grant, the Israel Science Foundation grant (1611/22), the Minerva Foundation, and the FEBS Foundation Excellence Award to MFP.

Author contributions

R.E., S.F., and M.F.P. conceived and designed the experiments. R.E. carried out the experiments. Y.L.K. conducted cryo-TEM measurements. All authors wrote the paper. R.E., S.F., Y.L.K., and M.F.P. contributed to the data interpretation. M.F.P supervised the research. All authors reviewed the paper.

Competing interests

The authors declare no competing interests.

Additional information

Supplementary information is attached.

Supplementary Files

This is a list of supplementary files associated with this preprint. Click to download.

- SupplementaryInformationFinalmfp.pdf